



HAL
open science

Sensitivity and resolution optimization in gas chromatography coupled to mass spectrometry analyses of volatile organic compounds present in vacuum environment

Ninette Abou Mrad, Steven Werner, Julie Mouzay, Grégoire Danger

► To cite this version:

Ninette Abou Mrad, Steven Werner, Julie Mouzay, Grégoire Danger. Sensitivity and resolution optimization in gas chromatography coupled to mass spectrometry analyses of volatile organic compounds present in vacuum environment. *Journal of Chromatography A*, 2020, 1609, pp.460489. 10.1016/j.chroma.2019.460489 . hal-03330160

HAL Id: hal-03330160

<https://hal.science/hal-03330160>

Submitted on 7 Mar 2022

HAL is a multi-disciplinary open access archive for the deposit and dissemination of scientific research documents, whether they are published or not. The documents may come from teaching and research institutions in France or abroad, or from public or private research centers.

L'archive ouverte pluridisciplinaire **HAL**, est destinée au dépôt et à la diffusion de documents scientifiques de niveau recherche, publiés ou non, émanant des établissements d'enseignement et de recherche français ou étrangers, des laboratoires publics ou privés.



Distributed under a Creative Commons Attribution - NonCommercial 4.0 International License

1 Sensitivity and resolution optimization in gas chromatography coupled to 2 mass spectrometry analyses of volatile organic compounds present in 3 vacuum environment

4 Ninette Abou Mrad^{1,2}, Steven Werner¹, Julie Mouzay¹ and Grégoire Danger^{1,*}

5 1. Aix-Marseille Université, CNRS, PIIM, UMR 7345, 13013 Marseille, France.

6 2. Université Paris-Sud 11, LETIAM, IUT d'Orsay, Plateau de Moulon, 91400 Orsay, France

7 *E-mail gregoire.danger@univ-amu.fr, phone number : +33491288285

8 Abstract

9 The gaseous phase analyses of *volatile organic compounds* (VOCs) are an important challenge
10 especially when these organics are formed in high vacuum environments (10^{-8} mbar) *reproducing the*
11 *environment of astrophysical ices formation and processing*. Several analytical techniques have been
12 developed to identify the molecular diversity formed from the processing of these ices. Among them,
13 the coupling of a GC-MS to the vacuum chamber where ices are processed highlighted the interesting
14 chemical diversity of such processed ices. These analyses were possible due to the development of a
15 specific system, the VAHIIA interface that enables the preconcentration of VOCs at low pressure (10^{-8}
16 mbar) and their transfer at higher pressure to the injection unit of a GC for their subsequent analyses.
17 This system showed sufficient repeatability (13%) and low detection limits (nmol) for simple ices [1],
18 but presents limits when ice mixtures are complex (*such as multi-component ices including water,*
19 *methanol and ammonia*). In this contribution, we present the optimization of our previous VAHIIA
20 system by implementing a cryofocusing system in the GC oven and by improving the recovery yield
21 of VOCs from the vacuum chamber to the VAHIIA interface. The cryofocusing provides an
22 improvement of efficiencies leading to higher resolution and signal to noise ratio, while the addition of
23 argon in the vacuum chamber during the VOC recovery allows increasing the amount of molecules
24 recovered by a factor of ~200. The coupling of both approaches provides an increase of sensitivity of a
25 factor ~400. At the end, experiments on astrophysical ices are shown demonstrating the interest of
26 such optimizations for VOC analyses.

27 Keywords

28 Volatile Organic Compounds, Vacuum environment, GC-MS, cryofocusing, ice analogs

29 1. Introduction

30 Direct and online analysis of Volatile Organic Compounds (VOCs) in vacuum environments using
31 chromatographic techniques is quiet problematic, mainly due to pressure differences between their
32 formation environments and the analytical instruments used for their analysis, to the compound
33 dilution that prevents direct analysis but also to delicate logistics to ensure online analysis preserving
34 the representativeness of samples. We addressed this issue in 2014 through the development of a

35 specific interface (referred to as VAHIIA) answering the main analytical challenges encountered in
36 such analysis, with a particular case application for VOCs coming from the photo and thermal
37 processing of astrophysical ice analogs formed in vacuum chambers mimicking the interstellar
38 medium [1]. We have earlier proposed to analyze qualitatively and quantitatively these VOCs by gas
39 chromatography coupled to mass spectrometry (GC-MS) [1,2], using the developed VAHIIA interface
40 that directly *connects* the vacuum chamber where compounds are formed (10^{-8} mbar) to the GC
41 injector (*higher than the atmospheric pressure*).

42 This VAHIIA interface is *composed* of two units. One is devoted to the VOCs recovery and their
43 preconcentration and is formed of a preconcentration loop (2.5 mL) *immersed* in liquid nitrogen. The
44 second unit allows the gaseous sample resulting from the preconcentration loop heating to be
45 introduced into the GC injector, and is constituted of gaseous injection loops (i.e. 500 μ L volume).
46 The VOCs transfer from the first unit to the second is realized following a controlled pressure
47 gradient, performed by increasing the pressure in the preconcentration loop after its warming relatively
48 to the injection loop through the addition of helium gas. Gaseous samples are then injected via the GC
49 injector. The VOC transfer from the vacuum chamber mimicking the interstellar medium to the GC is
50 reproducible (variability below 13%) with detection limits in the range of nanomolars [1].

51 *This VAHIIA interface was first used to characterize VOCs released in the gaseous phase from the*
52 *processing of a pure methanol ice. It enabled the detection of various compounds having different*
53 *chemical functions [2]. Thirty nine molecules having one to six carbon atoms were identified among*
54 *the hundred detected. However, the increase of the molecular diversity resulting from the increase of*
55 *the number of molecules composing the initial ice [3,4] brings up new challenges to overcome, both*
56 *for qualitative and quantitative measurements. Indeed, we observed low column theoretical plates for*
57 *peaks at low retention times, which implies low chromatographic resolution and column peak*
58 *capacity. In addition, the injection of a large sample volume (500 μ L) is a source of peak*
59 *broadening and therefore a decrease of efficiency.*

60 To overcome these drawbacks, we present herein the optimization of our previous VAHIIA system by
61 implementing a cryofocusing system inside the GC oven to limit the diffusion inherent to the injection.
62 Furthermore, to improve qualitative and quantitative aspects, we worked on the optimization of the
63 VOCs recovery from the vacuum chamber to the GC-MS by modifying the pressure inside the
64 chamber.

65 **2. Materials and Methods**

66 **2.1 Experimental set-up**

67 The basic equipment and techniques employed for the formation and the follow up of ice analogs have
68 been previously reported [1]. A brief description of the overall system is provided herein. All

69 experiments described were performed in a high vacuum chamber presenting a pressure of $5 \cdot 10^{-8}$ mbar
70 at 295 K and 10^{-8} mbar at 20 K. The gaseous methanol was deposited at a rate of 6×10^{-1} mol min^{-1}
71 on a copper-plated surface kept at 20 K with a closed helium cycle model 21 CTI cold head. In these
72 conditions an ice of methanol is formed on the sample holder. Control of sample is provided by
73 infrared spectroscopy [1]. The warming up of the ice mixture to room temperature was performed by
74 stopping the cryogenic system. For the VOC analysis, the chamber is connected to a GC-MS (GC
75 Trace **1310** and MS ion trap ITQ 900 from Thermofisher) with stainless steel tubes. *To test the impact*
76 *of the cryofocusing system, compounds were introduced in the gaseous form directly into the*
77 *preconcentration loop of the VAHIA interface and were not pumped from the vacuum chamber as*
78 *described in the introduction section. Details of the procedure are given elsewhere [1].*

79 The GC split/splitless (SSL) injector was maintained at 250 °C, and a split mode injection with a ratio
80 of 10 was conducted which ensures a good compromise between a high sensitivity while avoiding
81 column saturation. Separation of target analytes was achieved using a Rxi®-624 Sil MS (60 m \times 0.25
82 mm i.d. \times 1.4 μm d.f.) capillary column purchased from Restek, and using helium (alpha gaz 2) as the
83 carrier gas with a 1.18 mL min^{-1} constant flow rate. The temperature program started at 45 °C and was
84 held for 3 min. The temperature was then increased up to 150°C at a rate of 5°C min^{-1} , then to 220°C
85 at a rate of 20°C min^{-1} . The temperature of the transfer line from GC to MS was set at 250 °C. The ion
86 trap mass spectrometer was used in the electron impact ionization mode (ionization energy of 70 eV).
87 The ion source temperature was set to 250 °C and the maximum ion time in the trap was of 25 ms. The
88 signal was collected with a full scan mode in the mass range between 15 and 300 u . and a scan event
89 time of 0.16 s. For this study, the GC has been modified due to the addition of a gaseous sample
90 injection unit mainly constituted of sample loops detailed further in reference [1]. In addition, both
91 injectors have also been modified to allow gaseous sample injection. The first modification allows the
92 carrier gas to flush the sample injection loop at the injector level, and the second modification consists
93 of adding a stainless steel tube in the injector that brings the sample from the injection loop to the
94 injector [1]. The whole interest of having both these modified SSL injectors in our instrument is to
95 make possible the use of multiple columns for the analysis of molecular species having different
96 physical and chemical properties. Furthermore, column swapping is facilitated due to the use of a
97 vent-free GC/MS adapter (Frontier Laboratories LTD) (i.d. 0.15 mm, length ca 50 cm, column ultra-
98 ALLOY metal capillary) in the interface between the GC and the MS which limits the air flow into the
99 MS at values lower than 0.5 mL/min during the switching of columns. A MicroJet Cryo-Trap MJT-
100 1035E from Frontier Laboratories LTD was implemented on a 20 cm \times 0.25 mm i.d. Rxi guard
101 column from Restek. The cryogenic point was set at 10 cm from the head of the separative column.
102 Liquid nitrogen was used as a trapping gas allowing a cooling at the precolumn point around -190°C.

103 **2.2 Chemicals**

104 The VAHIA system was optimized using compounds belonging to different chemical classes *having*
105 *the main functional groups expected in the ice photoprocessing experiment*. For the laboratory
106 experiments, the standards of diethyl ether (anhydrous, assay $\geq 99\%$, ACS reagent), acetaldehyde
107 (puriss. p.a, anhydrous, assay $\geq 99.5\%$ (GC), Fluka), methyl acetate (anhydrous, assay 99.5%),
108 methanol (for pesticide residue analysis, Fluka Analytical), absolute methanol and acetonitrile (for
109 pesticide residue analysis, Fluka Analytical) were purchased from Sigma Aldrich, Saint Quentin
110 Fallavier, France.

111 **3. Results and Discussion**

112 **3.1 Cryofocusing to enhance resolution**

113 The main analytical challenge in the photo and thermal processing of astrophysical ice analogs comes
114 from the high molecular diversity obtained in such experiments. *As previously reported, the*
115 *photoprocessing of a pure methanol ice led to the formation of numerous alcohols, esters, ethers,*
116 *acids, ketones and aldehydes presenting a wide variability in volatility* [2]. Consequently, at the
117 minimum temperature of our GC oven (45°C), some molecules are not focused at the column head and
118 start to diffuse in the analytical column. These compounds present large peak widths implying weak
119 resolutions [5]. Furthermore, large sample volumes ($500\ \mu\text{L}$) are injected contributing to peak
120 broadening due to the extra-column dispersion effect. The objective is thus to trap analytes on a pre-
121 column in order to minimize peak broadening and increase peak capacity. Several techniques are used
122 to cryo-trap analytes in gas chromatography [6–9]. In the present work, the head of the *guard-column*
123 is cooled down to $77\ \text{K}$ *with a cryogenic controller injecting* a liquid nitrogen jet leading to the cryo-
124 focusing of analytes. If the cryogenic time is sufficient all analytes would be focalized. When trapping
125 is completed, analytes should be released from the *guard column* and introduced in a sharp band at the
126 head of the analytical column that would lead to higher column efficiency and better peak resolution.

127 The first step is to optimize the cryogenic time, which corresponds to the period during which the
128 liquid nitrogen flow is opened. For this purpose, three standards covering a range of saturated vapor
129 pressures *were introduced separately and directly into the preconcentration loop*: acetaldehyde (t_r :
130 $5.68\ \text{min}$), ethanol (t_r : $8.55\ \text{min}$) and ethyl acetate (t_r : $11.66\ \text{min}$) with various cryofocusing periods.
131 The evolutions of areas are statistically homogeneous (three injections for each period, $n=3$ with a
132 same injected quantity for each compound) whatever the cryo-focusing periods are, implying that the
133 system modification does not impact the compound recovery. Table 1 displays the evolution of
134 thermodynamic and kinetic factors as a function of the cryofocusing period. *The increase of retention*
135 *times observed with the cryofocusing compared to the non cryofocusing experiment is due to the*
136 *lapse of time where compounds are stacked at the cryogenic point on the guard column. This*
137 *cryofocusing time is the added to t_r' , and t_0 explaining this increase. As shown by the evolution of*
138 capacity factors (k'), compounds' retention on the stationary phase is not impacted by the

139 cryofocusing process since k' of all compounds are constant whatever cryogenic times are. Inversely,
140 data highlight an increase of column theoretical plates (N) with the increase of the cryofocusing
141 period, a phenomenon which is intimately related to the peak sharpening with cryofocusing. It is more
142 pronounced for analytes with low retention times since N of acetaldehyde increases by a factor of 11
143 while those of ethanol and ethyl acetate increase only by a factor of 4.5 and 2.5 respectively. The
144 difference observed between acetaldehyde and the two other compounds is due to their difference in
145 volatility. All compounds eluting between 4.3 min (column dead time) and 7.3 min (end of the 45°C
146 isotherm) are too volatile to get focused on the column head during the 3 min of isotherm at 45°C,
147 which is the case of acetaldehyde (5.68 min). These analytes diffuse and therefore present peak
148 broadening as observed in Figure 1. Once the cryofocusing operates, all analytes are trapped into a
149 thin plug at 77 K just after the injection. This phenomenon prevents the diffusion observed at 45°C,
150 which considerably increases N due to peak sharpening.

151 **Table 1** – Data related to the injection of specific standards to estimate the impact of the cryofocusing
152 on thermodynamic (capacity factor, k') and kinetic (column theoretical plates, N) factors. t_0 is obtained
153 from the air peak and RSD are obtained from 3 replicates ($n=3$). S/N_1 is the signal to noise ratio. k' is
154 *obtained by subtracting the cryofocusing time to the reduced retention time in order to only*
155 *consider the retention on the separative column.*

156 *We pursue our investigation by monitoring the evolution of the S/N_1 ratio as a function of the*
157 *cryofocusing period (Table 1). Data also show an S/N_1 increase once the cryofocusing is turned on*
158 *until it reaches a plateau at 45 s, which is related to N improvements. We then estimate a limit of*
159 *detection (LOD) by focusing on the lowest quantity (123 nmol, average RSD of 7% for triplicates) of*
160 *compounds injectable into the VAHIIA system (Table 2). By considering a S/N_1 of 3 at the LOD*
161 *value, estimated LOD were extrapolated for the 45s and the non-cryofocusing experiments.*
162 *Estimated LOD range from 0.3 to 6.2 nmol. The cryofocusing allows an average S/N_1 increase of 2*
163 *compared to the non cryofocusing method, resulting in lower detection limits.*

164 **Table 2** – Estimated LOD extrapolated from the lowest concentration (123 nmol) injectable in the
165 VAHIIA interface. S/N_1 at this concentration is displayed for diethyl ether, acetaldehyde and methanol
166 as well as the corresponding RSD ($n=3$). The estimated LOD is obtained by taking $S/N_1 = 3$ and
167 assuming a linear relation between our 123 nmol data and the $S/N_1 = 3$. The average RSD on areas is
168 7% showing a sufficient robustness.

169 To evaluate the impact of cryofocusing on the separation of VOCs, a mixture of six compounds (3
170 couples of compounds having close retention times) was injected using different cryofocusing periods
171 (from 0 s to 60 s, Figure 1). With no cryofocusing, column efficiencies for the first peaks are low
172 (Table 3) providing low resolution (0.42 between compounds 2 and 3, 1.00 between compounds 4 and
173 5, and 0.17 between compounds 6 and 7). When the cryofocusing is applied during 15 s, column

174 efficiencies for all compounds are highly increased with a higher impact for low retention time peaks.
175 Resolutions increase from 0.42 to 1.33 for compounds 2 and 3 and from 1.00 to 1.27 for compounds 4
176 and 5. At 45 s of cryogenic trapping, a significant improvement is observed with a complete resolution
177 reached between compounds 4 and 5. No improvements are observed at higher cryogenic times (60 s,
178 Figure 1). ***Our results pinpoint also the lower impact of cryofocusing on “high” retention time***
179 ***compounds tested in this study***, as observed for acetonitrile and methyl acetate which remain co-
180 eluted even though peak sharpening can be noted. Furthermore, the S/N_1 improvement with
181 cryofocusing allowed the detection of residual water for the first time. It is noticeable also that the
182 atmospheric carbon dioxide can also be resolved from the column dead time using cryofocusing even
183 if it does not interact with the column stationary phase. This resolution is only due to the retention of
184 carbon dioxide at 77 K at the cryofocusing position.

185 **Figure 1** – Effect of the duration of the cryofocusing on a standard mixture. Resolutions are calculated
186 from extracted ions of each compound. 1: O_2/N_2 column dead time, 2: acetaldehyde (m/z 43 u), 3:
187 methanol (m/z 31 u), 4: ethanol (m/z 45 u), 5: diethylether (m/z 59 u), 6: acetonitrile (m/z 41 u), 7:
188 methyl acetate (m/z 74 u). Note: Baselines of the different chromatograms are artificially shifted.
189 Same amounts of standards were injected at each experiment.

190 **Table 3** – Data related to Figure 1 displaying retention times (t_r), column theoretical plates (N) and
191 resolution (Rs) between acetaldehyde/methanol, ethanol/diethyl ether, acetonitrile/methyl acetate. Rs
192 and N are obtained from extracted ions: acetaldehyde (43), methanol (31), ethanol (45), diethyl ether
193 (59), acetonitrile (41), methyl acetate (74).

194 All these results demonstrate the impact of adding a cryofocusing trap to the VAHIA system. It
195 allows an important improvement of efficiencies, leading to better resolution and sensitivity.

196 **3.2 To improve the COV recovery from the vacuum chamber**

197 At another level, increasing the sensitivity of the VAHIA system required an improvement of the
198 VOC recovery yield from the vacuum chamber *where* ices are processed to the preconcentration loop
199 where VOCs are concentrated at 77 K. For this purpose, we investigated the impact of the pressure
200 inside the vacuum chamber on VOCs recovery. The experiment designed consisted of introducing 4
201 μmol of gaseous methanol inside the vacuum chamber (10^{-8} mbar), which condensed on the sample
202 holder maintained at 20 K. Once the vacuum chamber was isolated from the pumping system and the
203 sample holder warmed up to 300 K, the pressure in the vacuum chamber raised up to 10^{-3} mbar.
204 Ultrapure Argon was then added to reach various pressures in the chamber, and the resulting VOCs
205 recovery was monitored. Argon was used since it presents no chemical reactivity and since its freezing
206 temperature is of 40 K which prevents its condensation in the preconcentration loop at 77 K. Argon
207 was added to obtain a total pressure in the chamber of 10^{-2} , 10^{-1} , 1 or 10 mbar. Three experiments were

208 performed at each pressure to obtain an insight on the variability of VOCs recovery at a given
209 pressure. At 10^{-3} and 10^{-2} mbar, the area of methanol detected with the GC-MS is statistically
210 equivalent (Figure 2) and corresponds to a methanol recovery of 0.4%. However, once the pressure in
211 the chamber is increased to 10^{-1} mbar, the quantity of methanol recovered increases by a factor of 180
212 giving a 50% recovery of the initial methanol amount deposited in the vacuum chamber. The recovery
213 is even higher with a total pressure of 1 mbar, showing a 270-enhancement factor relatively to 10^{-3}
214 mbar, and remains stable with pressures higher than 1 mbar. At this total pressure in the vacuum
215 chamber around 80% of the initial amount of methanol is recovered.

216 **Figure 2** – Impact of the pressure inside the vacuum chamber on the amount of methanol recovered.
217 Error bars were calculated based on the standard deviation of methanol areas from replicates (n=3).

218

219 The increase in the amount of methanol recovered once the pressure in the chamber increases could be
220 related to the free molecular flow regime of gas that can occur at pressures below 10^{-2} – 10^{-3} mbar.
221 Once the pressure increases above 10^{-2} mbar, the free molecular flow evolves to a laminar flow where
222 argon drives a large part of gaseous species from the vacuum chamber to the preconcentration loop.

223 After both developments on VOCs recovery from the vacuum environment and VOCs cryofocusing
224 on the chromatographic column, we can estimate a total increase of the methanol sensitivity of a factor
225 about 400.

226 **3.3 Application to VOCs analysis coming from the photo- and thermal processing of a pure** 227 **methanol ice**

228 To test the impact of the previous optimizations on VOCs analysis, an ice of methanol was irradiated
229 during 24 h.

230 **Figure 3** – GC-MS analyses of the gases sublimated from a methanol ice sample after its irradiation
231 during 24 h. Chromatograms showing the impact of cryofocusing and pressure chamber increase are
232 displayed. 1: O₂/N₂ column dead time, 2: methanol, 4: acetone, 5: dimethyl ether, 6: acetaldehyde.
233 Note: Baselines of the different chromatograms are artificially shifted. *For a better reading, peaks 1,*
234 *CO₂ and 2 were manually truncated in the bottom and middle chromatograms. From 8.5 min the*
235 *intensity of the signal is multiplied by 3 in order to have a better insight on the remaining*
236 *compounds.*

237 The VOCs formed after the photo-processing of the methanol ice were transferred to the GC-MS
238 through the VAHIA interface using the new developments described in the previous section (Figure
239 3). In a first experiment, VOCs were recovered with no addition of Argon (final pressure after ice
240 warming of 10^{-3} mbar in the vacuum chamber) while using the cryofocusing (45 s). In comparison to

241 the experiment conducted with no cryofocusing published elsewhere [5], the cryofocusing allowed the
242 resolution of CO₂ from the column dead time and enabled the detection of H₂O. The second
243 experiment consisted in recovering VOCs with a 10 mbar pressure in the vacuum chamber with no
244 cryofocusing. An impressive increase in the number of detected compounds was observed as depicted
245 in the chromatogram (9-19 min) in Figure 3, with identifications of ethanol and acetone, next to H₂O
246 and methanol. As for the non photo-processed methanol used during the recovery optimization, the
247 VOCs recovery from samples presenting an important molecular diversity is also highly enhanced by
248 increasing the pressure in the vacuum chamber. The last experiment combined cryofocusing and
249 chamber pressure increase, resulting in a high number of detected species and a significant
250 improvement in sensitivity and resolution.

251 **4. Conclusion**

252 The introduction of cryofocusing to the VAHIA experimental set-up combined to the modification of
253 chamber pressure during VOCs recovery contribute clearly to enhance the detection sensitivity and to
254 improve chromatographic resolution. Consequently, our ability to detect new compounds in such
255 experiments increased in comparison to what has been developed previously. Indeed, our experimental
256 results pinpoint the presence of numerous new compounds that have not been previously observed, but
257 their identification is out of the scope of this work. Besides, the improvement of chromatographic
258 resolution enables the most possible non-ambiguous identification with mono dimensional
259 chromatography and low resolution mass spectrometry, and inevitably a reliable quantification. This
260 method optimization proved its effectiveness in the analysis of VOCs coming from a pure methanol
261 ice, and its contribution to the analysis of VOCs coming from the processing of complex ices is
262 without a doubt crucial to enlighten us on the composition of such gaseous samples.

263 **ACKNOWLEDGMENT**

264 This work has been funded by the CNRS programs "Programme National de Planétologie" (P.N.P,
265 INSU), "Programme de Physique et Chimie du Milieu Interstellaire" (P.C.M.I, INSU) and the "Centre
266 National d'Etudes Spatiales" (C.N.E.S) from its exobiology program. This work was further supported
267 by the ANR projects (VAHIA Grant ANR-12-JS08-0001, PeptiSystem grant ANR-14-CE33-0020,
268 and RAHIA_SSOM grant ANR-16-CE29-0015) of the French "Agence Nationale de la Recherche",
269 and by The Foundation of Aix-Marseille University.

270 **REFERENCES**

- 271 [1] N. Abou Mrad, F. Duvernay, P. Theulé, T. Chiavassa, G. Danger, Development and
272 optimization of an analytical system for volatile organic compound analysis coming from the
273 heating of interstellar/cometary ice analogues, *Anal. Chem.* 86 (2014) 8391–9.
274 doi:10.1021/ac501974c.

- 275 [2] N. Abou Mrad, F. Duvernay, T. Chiavassa, G. Danger, Methanol ice VUV photo- processing:
276 GC-MS analysis of volatile organic compounds, *Mon. Not. R. Astron. Soc.* 458 (2016) 1234.
277 doi:10.1093/mnras/stw346.
- 278 [3
- 279] G. Danger, F. Orthous-Daunay, P. de Marcellus, P. Modica, V. Vuitton, F. Duvernay, L.
280 Flandinet, L. Le Sergeant d'Hendecourt, R. Thissen, T. Chiavassa, Characterization of
281 laboratory analogs of interstellar/cometary organic residues using very high resolution mass
282 spectrometry, *Geochim. Cosmochim. Acta.* 118 (2013) 184–201.
283 doi:10.1016/j.gca.2013.05.015.
- 284 [4] A. Fresneau, N.A. Mrad, L. LS d'Hendecourt, F. Duvernay, L. Flandinet, F.-R. Orthous-
285 Daunay, V. Vuitton, R. Thissen, T. Chiavassa, G. Danger, Cometary Materials Originating
286 from Interstellar Ices: Clues from Laboratory Experiments, *Astrophys. J.* 837 (2017) 168.
287 doi:10.3847/1538-4357/aa618a.
- 288 [5] N. Abou Mrad, F. Duvernay, R. Isnard, T. Chiavassa, G. Danger, The Gaseous Phase as a
289 Probe of the Astrophysical Solid Phase Chemistry, *Astrophys. J.* 846 (2017) 124.
290 doi:10.3847/1538-4357/aa7cf0.
- 291 [6] B. Kolb, B. Liebhardt, L.S. Ettre, Cryofocusing in the combination of gas chromatography with
292 equilibrium headspace sampling, *Chromatographia.* 21 (1986) 305–311.
293 doi:10.1007/BF02311600.
- 294 [7] K. Watanabe-Suzuki, A. Ishii, O. Suzuki, Cryogenic oven-trapping gas chromatography for
295 analysis of volatile organic compounds in body fluids, *Anal. Bioanal. Chem.* 373 (2002) 75–
296 80. doi:10.1007/s00216-002-1240-z.
- 297 [8] J. Zhang, P. Zhang, H. Wang, Z. Pan, L. Wang, Analysis of volatile organic compounds in
298 pleural effusions by headspace solid-phase microextraction coupled with cryotrap gas
299 chromatography and mass spectrometry, *J. Sep. Sci.* 39 (2016) 2544–2552.
300 doi:10.1002/jssc.201600279.
- 301 [9] T.P. Wampler, E.J. Levy, Cryogenic focusing of pyrolysis products for direct (splitless)
302 capillary gas chromatography, *J. Anal. Appl. Pyrolysis.* 8 (1985) 65–71.

303

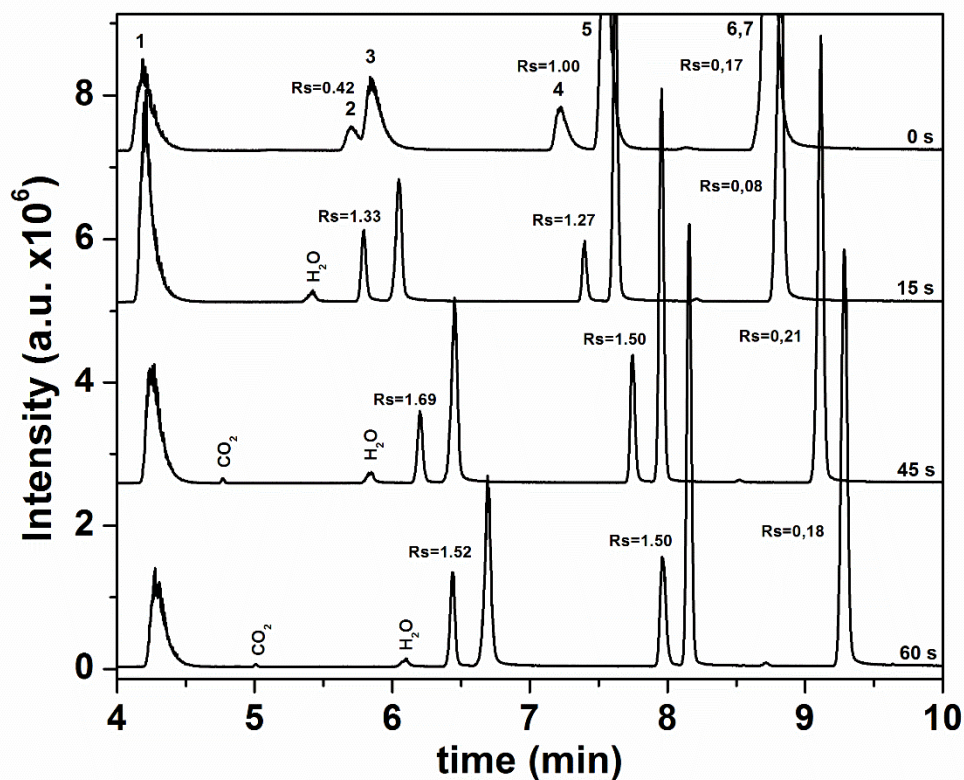


Figure 1 – Effect of the duration of the cryofocusing on a standard mixture represented by the total ion current. Resolutions are calculated from extracted ions of each compound. 1: O₂/N₂ column dead time, 2: acetaldehyde (m/z 43 u), 3: methanol (m/z 31 u), 4: ethanol (m/z 45 u), 5: diethyl ether (m/z 59 u), 6: acetonitrile (m/z 41 u), 7: methyl acetate (m/z 74 u). Note: Baselines of the different chromatograms are artificially shifted. Same amounts of standards were injected at each experiment.

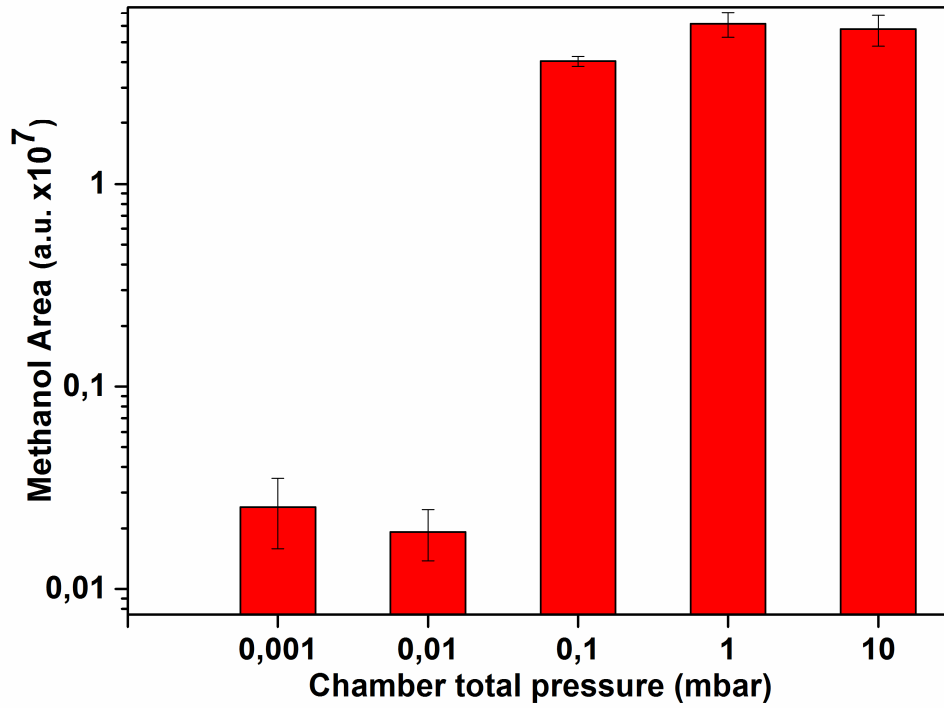


Figure 2 – Impact of the pressure inside the vacuum chamber on the amount of methanol recovered. Error bars were calculated based on the standard deviation of methanol areas from replicates (n=3).

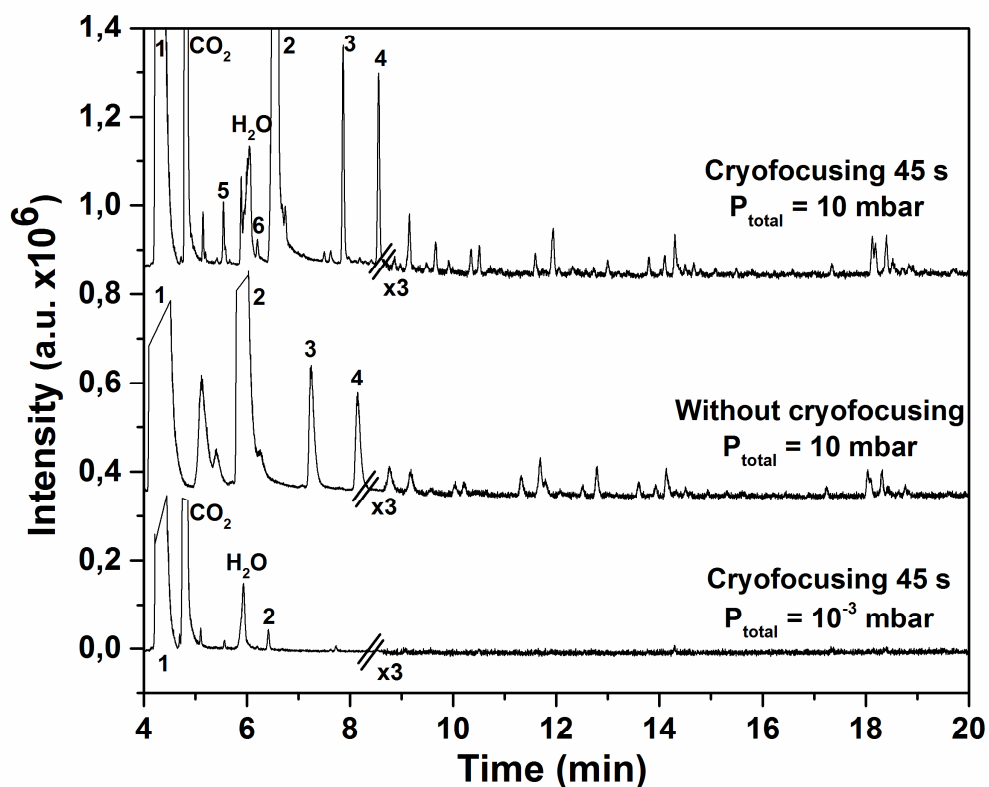


Figure 3 –GC-MS analyses of the gases sublimated from a methanol ice sample after its irradiation during 24 h. Chromatograms showing the impact of cryofocusing and pressure chamber increase are displayed. 1: O₂/N₂ column dead time, 2: methanol, 4: acetone, 5: dimethyl ether, 6: acetaldehyde. Note: Baselines of the different chromatograms are artificially shifted. **For a better reading, peaks 1, CO₂ and 2 were manually truncated in the bottom and middle chromatograms. From 8.5 min the intensity of the signal is multiplied by 3 in order to have a better insight on the remaining compounds.**

Table 1 – Data related to the injection of specific standards to estimate the impact of the cryofocusing on thermodynamic (capacity factor, k') and kinetic (column theoretical plates, N) factors. t_0 is obtained from the air peak and RSD are obtained from 3 replicates ($n=3$). S/N_1 is the signal to noise ratio. k' is obtained by subtracting the cryofocusing time to the reduced retention time in order to only consider the retention on the separative column.

	Cryo time (s)	t_0 ¹ (min)	t_r (min)	RSD ² (t_r) (%)	k'^3	N (10^6)	RSD (N) (%)	S/N_1 ⁴	RSD (S/N_1) (%)
Acetaldehyde	0	4.16	5.68	0.10	0.36	14	4	159	27
	5	4.18	5.71	0.10	0.36	30	5	450	5
	15	4.20	5.82	0.17	0.36	107	24	497	14
	30	4.22	6.06	0.19	0.35	120	18	465	14
	45	4.22	6.29	0.24	0.35	130	18	543	11
	60	4.24	6.54	0.23	0.34	155	16	561	13
Ethanol	0	4.19	7.24	0.08	0.72	23	5	230	15
	5	4.16	7.32	0.00	0.74	47	12	336	14
	15	4.17	7.41	0.00	0.73	79	10	325	7
	30	4.19	7.61	0.13	0.72	81	5	323	12
	45	4.23	7.82	0.07	0.71	101	6	313	12
	60	4.23	7.98	0.12	0.71	89	12	318	2
Methyl acetate	0	4.21	11.66	0.05	1.77	144	5	782	17
	5	4.19	11.67	0.05	1.78	306	1	1398	4
	15	4.18	11.74	0.10	1.79	356	13	1258	13
	30	4.22	11.85	0.00	1.76	333	13	1633	10
	45	4.22	11.95	0.05	1.73	365	1	1541	10

¹ t_0 is obtained from the air peak.

² RSD are obtained from 3 replicates ($n=3$).

³ k' is obtained by subtracting the cryofocusing time to the reduced retention time in order to only consider the retention on the separative column.

⁴ S/N_1 is the signal to noise ratio.

Table 2 – Estimated LOD extrapolated from the lowest concentration (123 nmol) injectable in the VAHIA interface. S/N_1 at this concentration is displayed for diethyl ether, acetaldehyde and methanol as well as the corresponding RSD (n=3). The estimated LOD is obtained by taking $S/N = 3$ and assuming a linear relation between our 123 nmol data and the $S/N_1 = 3$. The average RSD on areas is 7% showing a sufficient robustness.

	Cryofocusing	S/N_1	RSD (%)	Estimated LOD (nmol) $S/N_1 = 3$
Diethyl ether	OFF	623	9	0.6
	45 s	1250	15	0.3
Acetaldehyde	OFF	218	5	1.7
	45 s	519	8	0.7
Methanol	OFF	59	16	6.2
	45 s	99	17	3.9

Note: S/N_1 were derived from the Xcalibur software

Table 3 – Data related to Figure 1 displaying retention times (t_r), column theoretical plates (N) and resolution (Rs) between acetaldehyde/methanol, ethanol/diethyl ether, acetonitrile/methyl acetate . Rs and N are obtained from extracted ions: acetaldehyde (43), methanol (31), ethanol (45), diethyl ether (59), acetonitrile (41), methyl acetate (74).

Cryo time (s)	Compound (Extracted ion)	t_r (min)	N	Rs
0s	Acetaldehyde (43)	5.70	2140	0.42
	Methanol (31)	5.84	1380	
	Ethanol (45)	7.22	2651	1.00
	Diethyl ether (59)	7.55	2899	
	Acetonitrile (41)	8.68	3610	0.17
	Methyl acetate (74)	8.73	6755	
15s	Acetaldehyde (43)	5.79	5732	1.33
	Methanol (31)	6.05	4598	
	Ethanol (45)	7.40	9363	1.27
	Diethyl ether (59)	7.61	14259	
	Acetonitrile (41)	8.79	5089	0.08
	Methyl acetate (74)	8.81	11911	
45s	Acetaldehyde (43)	6.20	12601	1.69
	Methanol (31)	6.47	6424	
	Ethanol (45)	7.76	19739	1.50
	Diethyl ether (59)	7.97	15640	
	Acetonitrile (41)	9.40	23406	0.21
	Methyl acetate (74)	9.13	23561	
60s	Acetaldehyde (43)	6.44	15955	1.52
	Methanol (31)	6.69	5622	
	Ethanol (45)	7.94	15522	1.50
	Diethyl ether (59)	8.15	21774	
	Acetonitrile (41)	9.26	11876	0.18
	Methyl acetate (74)	9.29	24394	